RSC Advances

ROYAL SOCIETY OF CHEMISTRY

www.rsc.org/advances

Journal Name

ARTICLE

Cationic benzylidene cyclopentanone photosensitizers for selective photodynamic inactivation of bacteria over mammalian cells

Received 00th January 20xx,
Accepted 00th January 20xx

DOI: 10.1039/x0xx00000x

www.rsc.org/

Yanyan Fang,[a, b] Tianlong Liu,[a] Qianli Zou,[a] Yuxia Zhao*[a] and Feipeng Wu*[a]

To inactivate both standard strains as well as antibiotic-resistant strains with minimum damage to host cells, three new pyridyl cationic-modified benzylidene cyclopentanone photosensitizers (PSs), **P1** (with one cationic group), **P2** (with two cationic groups bilaterally), and **P3** (with two cationic groups unilaterally) were synthesized and characterized. Their selective uptakes by bacteria over HepG2 cells and their photodynamic inactivation efficiencies against *Staphylococcus aureus* (ATCC 6538), *Escherichia coli* (ATCC 25922), and the drug-resistant *Escherichia coli* (CA-31) were studied using methylene blue (**MB**) and hematoporphyrin monomethyl ether (**HMME**) as references. The results showed that the uptake amounts of **P1**, **P2**, and **P3** by all strains were at least 2, 20, and 18 times more than those by HepG2 cells, respectively. All PSs exhibited good antimicrobial photodynamic therapy (aPDT) effects towards three strains with low concentrations of ≤ 8.0 μM, while **MB** was invalid towards three strains and **HMME** was invalid toward *Escherichia coli* (CA-31) with the concentration up to 32.0 μM. Especially, the minimum inhibitory concentrations (MICs) of **P3** against these strains were all ≤ 2.0 μM, under which about 94% HepG2 cells were still alive, indicating **P3** had high aPDT selectivity for bacterial cells over mammalian cells. The relationships between structure and antimicrobial properties of these cationic PSs were discussed to reveal their high photodynamic inactivation selectivity of bacterial cells.

1. Introduction

The discovery of antibiotics has greatly enhanced the abilities of humans to resist microbial infections. However, the worldwide rapidly increasing antibiotic resistance among pathogenic bacteria is becoming a serious problem.[1] In this regard, photodynamic therapy (PDT),[2, 3] a powerful clinical protocol for the treatment of tumors, has been proposed as a promising alternative method to inactivate bacteria, viruses, fungi, and protozoa.[4, 5] Unlike antibiotics, in antimicrobial PDT (aPDT) process, photosensitizer (PS) is irradiated to generate reactive oxygen species (ROS), such as superoxide ($O_2^{\cdot-}$), hydroxyl radical ($HO^{\cdot}$) and/or singlet oxygen ($^1O_2$) to kill microbial cells.[6, 7] The multi-target nature and non-involvement of the genetic material property of aPDT make it less chance to induce the bacterial resistance or trigger the bacterial repair mechanisms.[8-11] In recent years, aPDT has proved its potential in disinfection of contaminated blood[12] and environmental waters.[13]

Generally, Gram-positive (Gram-(+)) bacteria are more sensitive to aPDT because their outer walls are relatively porous and all types of PSs can diffuse through them readily.[14] Instead, Gram-negative (Gram-(−)) bacteria have an additional, more negatively charged outer layer that serves as a permeability barrier to prevent the entry of noxious compounds.[15] For this reason, neutral and anionic PSs are often failed to inactivate Gram-(−) bacteria effectively while cationic PSs can still bind to their outer membrane strongly and damage their integrity.[16-19] Therefore, cationic PSs are considered to be broad-spectrum antimicrobial agents having more potential for the development of aPDT.

For an ideal aPDT process, the bacterial cells should be selectively inactivated with low or even no PDT damage to host tissues.[16] One strategy to achieve this goal is to combine photoactive compounds with bacteria-targeted agents or carriers. In previous studies, Friedberg et al.[20] reported that binding PSs to a monoclonal antibody (Mab) could specifically kill *P. aeruginosa*. Gross et al.[21] obtained a highly selective aPDT against *Staphylococcus aureus* by linking a PS with a non-specific IgG. However, the broad-spectrum antimicrobial potencies of these PSs showed decreases after such modifications. Another strategy to promote selectivity is to take advantage of the differences in membrane composition and transmembrane potential between bacterial cells and mammalian cells. As some studies revealed, the negative transmembrane potential in bacterial cells was much higher than that in mammalian cells, and more importantly, the negative charges were located on the outer wall of bacteria but in the inner leaflets of mammalian cells.[19] Recently, Zhu et

[a] Technical Institute of Physics and Chemistry, Chinese Academy of Sciences, Beijing 100190, P. R. China. E-mail: yuxia.zhao@mail.ipc.ac.cn; Tel: +86 10 82543532; E-mail: fpwu@mail.ipc.ac.cn; Tel: +86 10 82543569, Fax: +86 10 82543491.
[b] University of Chinese Academy of Sciences, Beijing 100049, P. R. China.
† The authors declare no competing financial interest.

al.[22] reported that a cationic conjugated polymer with a relatively high quaternary ammonium ratio could selectively combine with bacterial cells but did not bind to Jurkat T cells, indicating that the membrane charge difference between bacteria and mammalian cells was large enough to be clearly distinguished by cationic PSs.

In our previous studies, we reported two series of water-soluble benzylidene cyclopentanone PSs modified by polyethylene glycol (PEG) and carboxylate anionic groups, and proved that several of them were good candidates for anticancer PDT.[23, 24] Moreover, we found that the anticancer PDT effects of these PSs sharply decreased with their increasing hydrophilicity, and proved that this was related to their decreased uptake by mammalian cells. Here, we design three novel pyridyl cationic-modified benzylidene cyclopentanone PSs (**P1**–**P3**, shown in Figure 1). By introducing different numbers of pyridyl cationic groups at different positions, we expect that the uptake capabilities of these PSs by bacteria will be significantly affected, and the detailed structure-antimicrobial property relationships of these cationic PSs are analysed and discussed. The significant photodynamic inactivation efficiencies of these PSs against the Gram-(+) *Staphylococcus aureus* (*S. aureus*, ATCC 6538), Gram-(–) *Escherichia coli* (*E. coli*, ATCC 25922), and drug resistant strain *E. coli* (CA-31) are studied. Methylene blue (**MB**),[25-28] one of the most widely used cationic PS in clinical practice right now, and hematoporphyrin monomethyl ether (**HMME**),[29-31] an effective second-generation anionic PS, which has been used in the treatment of various clinical diseases for years, are used as reference compounds. What's more, the high selective photodynamic inactivation of these PSs towards bacteria over mammalian cells is studied and analysed.

2. Experimental

2.1. Synthesis and characterization. The synthesis routes of photosensitizers (**P1**–**P3**) are shown in Scheme 1. All final compounds were characterized by ^{1}H NMR spectra, HR-MS, element analysis, and HPLC analysis confirming a purity of >95%. **DEA** was synthesized and reported in our previous work.[23]

2.2. Fluorescence quantum yield. The fluorescence quantum yields of **P1**–**P3** in PBS were measured using the fluorescein disodium salt as reference (Φ_f = 0.9).[32]

2.3. Singlet oxygen production. The singlet oxygen quantum yields (Φ_Δ) of **P1**–**P3** were measured using 9,10-anthracenediyl-bis(methylene)dimalonic acid (AMDA) and Rose Bengal as $^1O_2$ scavenger and the reference, respectively.[33] The experimental details are given in supporting information.

2.4. Bacterial growth. In this study, the Gram-(+) *S. aureus* (ATCC 6538), Gram-(–) *E. coli* (ATCC 25922) and a drug resistant strain, β-lactamase producing *E. coli* (CA-31), which was isolated from swine and provided by the College of veterinary, China Agricultural University, were selected as study subjects. Both *S. aureus* and *E. coli* were revived with Luria Bertani (LB) broth and nutrient agar at 37°C for 24 hours. The OD600 value, the optical density at 600 nm, was monitored to determine the density of bacterial cells.

2.5. The uptakes of PSs by bacterial cells. For the uptake test, a bacterial suspension (~ 10^8 CFU per mL) of each strain with 10 μM PSs was prepared. After 1 h of incubation in dark at room temperature, the suspension was centrifuged at 5000 rpm for 10 min to harvest the bacteria. The obtained bacteria were washed with PBS for three times and then lysed with lysozyme (100 μg/mL) for 1h followed by sonication for 2h at 37°C. The lysed bacterial solution was centrifuged again to obtain the supernatant. The fluorescence intensity of the samples was measured, excited at 460 nm and monitored from 475 nm (for methylene blue, excited at 580 nm and monitored from 595 nm). The fluorescence intensity of PSs at the concentration of 10 μM without bacteria was taken as the baseline for the calculation of the uptake amount.

2.6. Agarose diffusion assay. The agarose diffusion assay was used to analyse the antibacterial PDT activity of PSs, *S. aureus*, *E. coli* and the drug resistant strain *E. coli* (CA-31) were used as the test organisms. According to the method reported by Lehrer et al.[34], 3 mL cell suspensions (~ 10^5 CFU per mL) were added into 100 mL of warmed (50°C) agarose, then poured into a sterile Petri dish (Φ = 10 cm) and allowed to harden. A sterile puncher (diameter ~ 4.5 mm) was used to bore holes, and then 20 μL samples at six different concentrations of 4.0, 8.0, 16.0, 32.0, 50.0 and 64.0 μM were added to each well. After incubating the plates upright at 37°C for 1 h, the control group (without light) was put into the incubator for continuous incubation. For the experimental group, a 532 nm laser (30 J cm^{-2}, 10 min) was used to irradiate each hole for 10 min. The inhibition zones of both the control group and the experimental group were evaluated after another 24 h of incubation at 37°C in the dark.

2.7. Minimum inhibitory concentration (MIC) test. In MIC test, a modified resazurin method reported by Elavarasan et al. was utilized.[35] As shown in the schematic diagram (Figure S2), the concentrations of four neighboring wells in a sterile 96-well plate, for example C1, C2, D1, and D2, are same. 100 μL of the photosensitizers at different concentrations were added into the corresponding wells on 96-well plates. The **GM** group (100 μL 1% gentamicin in each well) and the **B+B** group (100 μL broth with bacteria) were used as the positive-control and negative-control groups, respectively. All the wells described above contained 10 μL of bacterial suspension (~ 5×10^6 CFU per mL) to achieve a final concentration of 5×10^5 CFU per mL except of the **Broth** group, which contained 10 μL of nutrient broth as the blank-control group. These 96-well plates were irradiated with a 532 nm laser for 10 min (the total light dose was approximately 30 J cm^{-2}) and incubated at 37°C for another 18 h. For methylene blue, a 635 nm laser (30 J cm^{-2}) was used. A 0.0675% resazurin solution was prepared. 10 μL of resazurin indicator solution was added into each well and then plates were incubated at 37°C. After 4 h of chromogenic reaction, the lowest concentration showing no pink colour

change was considered as the complete growth inhibition concentration of a PS. Each test was carried out for three times at different days. The relative death rate was calculated by equation (1) after monitoring the optical density (OD) value of each well at 630 nm.

$$\text{Relative death rate } (\%) = \left(1 - \frac{OD_2 - OD_0}{OD_1 - OD_0}\right) \times 100\% \quad (1)$$

Where OD_0, OD_1, and OD_2 are the average OD values of **Broth** group, **B+B** group, and experimental group, respectively. The data of **GM** group was used as reference to normalize the results.

2.8. Cell culture. HepG2 cells and mouse melanoma B16 cells were cultured with the growth media (DMEM supplemented with 10% FBS, 100 unit/mL penicillin, 100 μg/mL streptomycin at 37°C in a humidified atmosphere containing 5% CO_2). All the PSs were dissolved in PBS (pH=7.4), as 1.0 mM stock solutions, and then diluted in the growth media to the final working concentrations.

2.9. The uptakes of PSs by HepG2 cells. The HepG2 cells were incubated with 10 μM PSs in 12-well plates for certain hours, and then, after washing the cells with PBS for three times, 200 mL lysis buffer (20 mM Tris, pH 7.5, 150 mM NaCl, 1% Triton X-100) was used to lyse the cells.[36] The intracellular concentration of PSs at different incubation times was calculated based on the measurement of fluorescence intensity.

2.10. Subcellular localization. To detect the subcellular localization, a confocal laser scanning microscope (Nikon AIR MP) was used. HepG2 cells were incubated in a cover glass chamber (diameter 35 mm) for 24 h to reach a density of 1×10^5 cells per well. Media containing 10 μM PSs was used to replace the original culture solution. After 8 h incubation, the chambers were washed with PBS for three times. Then the culture media with 100 nM Mito-tracker green was used to incubate the cells for 20 min and the chambers were washed with PBS again. A light of 488 nm was used to excite Mito-tracker green, while the PSs were excited by a 561 nm light.

2.11. Cytotoxicity of PSs. For the dark cytotoxicity, HepG2 cells and B16 cells were dispersed and cultured in 96-well plates for 24 h. Then, 100 μL culture media containing different concentrations of PSs were used to replace the original culture solution. After another 24 h of incubation, the cell viability was determined by CCK-8 assay. For photo-cytotoxicity, a 532 nm laser (30 J cm^{-2}, 10 min) was used to irradiate the cells after incubating them with PSs for 8 h. Then, after 10 min irradiation, the cells were incubated in the dark for another 24 h before testing. Cells without PSs were also treated with the same laser and were used as the 100% cell survival base line.

2.12. Statistical analysis. Independent assays and replicates of the same sample were done to obtain the representative results. Data were statistically analyzed by one-way analysis of variance (ANOVA) test using SPSS 16.0 (SPSS Inc., Chicago, IL). The p value of <0.05 was considered to be statistically significant.

3. Results and discussion

3.1. Synthesis and characterization. Scheme 1 shows the synthetic route of **P1**, **P2**, and **P3**. Compounds **C1** and **C2** containing one or two chlorinated ethyl groups were synthesized via a Vilsmeier-Haack reaction of the hydroxyl groups in **B1** and **B2** with phosphorus chloride and DMF according to the report of Massin et al.[37] Intermediate products **D1–D3** were obtained in excellent yields (90–95%) via a base-catalysed condensation reported in our previous work.[23] The final target cationic PSs were synthesized by the alkylation of pyridine with **D1–D3**. Purifications of these cationic PSs were achieved by re-crystallization from toluene, and the characterization data, including ^{1}H NMR, HR-MS, elemental analysis and HPLC spectra of these PSs, are provided in supporting information.

3.2. Solubility and octanol-water partition coefficient. As data shown in Table 1, after introducing one or two pyridyl groups, the water solubility of all PSs **P1–P3** (> 4 mg mL^{-1}) is significantly improved compared with the prototype compound 2,5-bis(4-(diethylamino)benzylidene cyclopeantanone (**BDEA**).[23] Additionally, the water solubility enhances with the increasing number of pyridyl groups. The Log P values are 1.8 for **P1**, −1.0 for **P2**, and −0.1 for **P3**, respectively. It is interesting that the Log P values of these PSs are affected not only by the number of the pyridyl groups, but also by the position of the modification. **P2**, bilaterally modified by two pyridyl groups is less lipophilic than **P3** modified unilaterally. For **P3** still has one lipophilic end, it may make it easier to enter the lipid phase. In this study, the Log P values of **MB** and **HMME** were also measured as 0.1 and 0.8, respectively.

3.3. Photophysics and singlet oxygen production. The absorption and fluorescence emission properties of all PSs were carried out in PBS (phosphate buffered saline) (Table 1). As shown in Figure 2, the absorption and emission bands both blue-shift from **P1** to **P2** and **P3**, which indicates that the electron-donating capability of the terminal dialkyl-amino group decreases after modification by the pyridyl cationic group. Compound **P2** exhibits the largest absorption band gap because its two terminal amino groups are affected.

As results shown in Table 1 and Figure S3, the Φ_Δ values of **P1** and **P3** are 0.036 and 0.027, respectively, and no significant changes are found when increasing the number of unilaterally modified groups. Compound **P2**, which is bilaterally modified by two pyridyl groups, has an obviously reduced Φ_Δ value (0.007), likely as a result of its enhanced radiative transition of fluorescence emission (Table 1).

3.4. The uptakes of PSs by bacterial cells. Bacteria cellular uptake was examined by incubating suspensions of Gram-(+) *S. aureus*, Gram-(−) *E. coli*, and the drug resistant strain of *E. coli* (CA-31) with PSs, respectively, at the concentration of 10 μM in dark for 1 h. After centrifugation to remove the supernatant, the bacterial cells were lysed and the fluorescence intensity of these PSs in the lysed solution was detected. As shown in Figure 3, **P1**, **P2**, and **P3** are taken up by the three strains more readily than **MB** and **HMME**, and the difference is significant (P

< 0.05). Moreover, the order of uptake amount is the same as **P3** > **P2** > **P1** > **MB** ≈ **HMME** in all these strains. For example, the uptake amounts of **P1**, **P2**, **P3**, **MB**, and **HMME** by *S. aureus* are 1003, 1308, 1457, 236, and 189 pmol/10^6 cells, respectively, and by *E. coli* (CA-31), they are 434, 765, 1200, 46, and 15 pmol/10^6 cells, respectively. As expected, the positive charges in cationic PSs enhance their electrostatic interaction with the negatively charged outer membranes of bacteria, so it is reasonable to find that the uptake amounts of cationic PSs **P1–P3** are more than those of the anionic PS **HMME**, and the uptake of **P2** and **P3**, with two cationic groups, are higher than that of **P1** with one cationic group. However, the large difference of uptake between **P1** and **MB** indicates that the charge is not the only determinant. It seems that the bacteria cellular uptake also correlated with the Log P value of these PSs, so **P1** with the higher Log P (1.8) is taken up more than **MB** (Log P = 0.1) by bacteria, and a similar trend is also found when comparing **P3** with **P2**. Additionally, owing to the enhanced efflux pump function and the more strict control of outer membrane permeability in drug resistant strains,[38] the uptake amounts of PSs by *E. coli* (CA-31) are the lowest when compared with the corresponding data obtained for the other two strains. **P3**, the PS taken up the best by all three strains, is promising as a potential anti-bacteria agent.

3.5. Antimicrobial PDT. Inhibition zones tests were carried out at six different concentrations. The results are listed in Table S1 and partly shown in Figure S5. A typical result with PSs as 4.0 μM is shown in Figure 4. Under the light conditions (532 nm, 30 J cm^{-2}, 10 min), it is clear that no obvious bacterial cell death is found in the blank groups. However, for the experimental groups, **P1**-**P3** showed obvious antibacterial abilities even without light, and these results were consistent with the natural antibacterial property of cationic PSs.[39, 40] **P3** has the best aPDT effect because of its higher bacterial uptake efficiency, although its Φ_Δ value is a little lower than that of **P1**. Additionally, despite its more effective uptake results, **P2** has inferior aPDT effects compared with **P1** because of its obviously decreased Φ_Δ value.

For quantitative evaluation, the MIC assay was carried out using a modified resazurin method. The relative death rate of the bacterial cells was calculated by monitoring the optical density of the wells at 630 nm (Figure 5). The wells in which the blue color did not turn to pink were considered to correspond to the MIC, and the relative death rate of **GM** group (> 97%) was used as references. A 532 nm laser (30 J cm^{-2}) was used to irradiate **P1–P3** and **HMME**, and a 635 nm laser (30 J cm^{-2}) was used for **MB**. The results are shown in Table 2 and Figure S6, **P1–P3** (MIC ≤ 8 μM) exhibits more excellent aPDT effects than those of **MB** (MIC > 32 μM) against *S. aureus*, *E. coli*, and even the drug resistant strain of *E. coli* (CA-31). Though **MB** has much higher Φ_Δ value (~ 0.5 in PBS[41]) than those of **P1–P3**, its lower uptake amounts will limit its effect. Moreover, as reported previously, **MB** could readily form dimmers on the bacterial cell surface, which would sharply decrease its ability to photo-inactivate microbes.[42]

For *S. aureus* and *E. coli*, the photodynamic inactivation abilities of **P1–P3** are close to or equivalent to **HMME**. The MIC values of **P1**, **P2**, **P3**, and **HMME** against *S. aureus* are 2.0, 2.0, 1.0, and 1.0 μM, respectively, while against *E. coli*, they are 4.0,
4.0, 2.0, and 2.0 μM, respectively. It is worth to mention that although **HMME** is an anionic PS, its activity to inactivate Gram-(−) *E. coli* is still comparable to the cationic PSs, **P1–P3**, which is likely as a result of its advantage of relatively high Φ_Δ values (~ 0.13 in PBS[43]). However, for the drug resistant strain *E. coli* (CA-31), the photodynamic inactivation ability of **HMME** is significantly decreased (MIC > 32 μM), and this MIC is significantly different with those toward *S. aureus* and *E. coli* (P < 0.05). The more strict control of the outer membrane permeability against the entrance of noxious compounds and the enhanced ability of the efflux pump are likely explanations.[38]

Most interestingly, the cationic PSs **P1–P3** show obvious antimicrobial properties against not only standard strains but the antibiotic resistant strain *E. coli* (CA-31), especially for **P3**, which is the best among all three newly synthesized cationic PSs. The reasons for the effective antimicrobial PDT effects of these cationic PSs include both the destructive effect of $^1O_2$, and the destabilization and interruption of native organized bacterial cell walls caused by cationic charges.[44]

3.6. The uptakes of PSs by HepG2 cells and their subcellular localization. To evaluate the safety of these cationic PSs towards mammalian cells, the test of cellular uptake and subcellular localization toward HepG2 cells was carried out. HepG2 cells were incubated with PSs for 1, 2, 4, 6, 8, 12 and 24 h, respectively. The results are shown in Figure 6. The concentrations of the three PSs in cells reach a plateau after 8h incubation. Because of its relatively high Log P value, the mono-cationic PS **P1** accumulates the most in cells. However, the uptake process is hindered when there is more than one cationic group in the PS. The amounts of **P2** and **P3** taken up by the cells are much lower compared with **P1**, which is also demonstrated by the images of subcellular localization obtained by confocal laser scanning microscope (CLSM).

Although the numbers of modified groups in **P2** and **P3** are the same, **P3**, modified unilaterally, possesses a higher rate of uptake compared with that of **P2** (modified bilaterally). This subtle change may be attributed to the high lipophilicity of the unilateral bis-ethyl agents in **P3** favoring to the cellular uptake process. The uptake amounts of **P1**, **P2**, and **P3** are 190, 38, and 67 pmol/10^6 cells, respectively, after incubating HepG2 cells with 10 μM PSs for 1 h. It is worth to mention that the uptake amounts of **P1**, **P2**, and **P3** by the three strains are at least about 2, 20, and 18 times more than that by HepG2 cells under parallel conditions (10 μM PSs in dark for 1 h). The high selectivity of **P2** and **P3** for bacterial cells over HepG2 cells indicates the possibility for such PSs to selectively inactivate bacterial cells with low PDT damage to host tissues.

Additionally, as shown in Figure 6b, **P1** accumulates mainly in mitochondria, the cellular energy manufacturing factory,

indicating its high photo-cytotoxicity toward HepG2 cells. **P2** and **P3** accumulate mainly in cell membranes. Compared with the size of mammalian cells (~ 20 μm), the lifetime and the action radius of $^1O_2$ is short in biologic systems (<0.04 ms and < 0.02 μm),[45] so the damages of PSs **P2** and **P3** toward important organelles inside cells are limit.

3.7. Cytotoxicity of PS. To further understand cytotoxicities of these cationic PSs, the dark- and photo-cytotoxicity of them toward HepG2 cells were studied. As shown in Table 2 and Figure 7, both **P2** and **P3** show negligible dark-cytotoxicity towards HepG2 cells at the concentrations up to 40 μM. However, the cytotoxicity of **P1** in the dark (IC_{50}(dark)= 33.5μM) is relatively significant ($P < 0.05$, compared with the results of **P2** and **P3**), likely as a result of its high cellular uptake. From the photo-cytotoxicity study, the IC_{50}(light) value of **P1** (4.4 μM) was relatively low compared with those of **P2** (9.6 μM) and **P3** (7.7 μM). Obviously, **P1** shows less chance to be considered as an effective aPDT agent because its MIC value to photo-inactivate *E. coli* (CA-31) is as high as 8.0 μM and only 21% of HepG2 cells are detected to survive at this concentration. Although **P3** seems more toxic than **P2** owing to its Φ_Δ value and cellular uptake efficiency, it is the most likely candidate for aPDT after taking its antimicrobial results as well as dark- and photo-cytotoxicity towards HepG2 cells into consideration. At 8.0 μM (the MIC for **P2** to photo-inactivate *E. coli* (CA-31)), the cell viability of **P2** towards HepG2 cells was about 68% after irradiation. By comparison, about 94% of HepG2 cells still survive at the MIC value of **P3** (all $\leq$ 2.0 μM), which indicates that bacterial cells can be selectively photo-inactivated while minimizing the damage to mammalian cells. This selectivity is further confirmed by B16 cells, a cell line from skin. As shown in Figure S7, the IC_{50}(light) values of **P1**, **P2**, and **P3** are 4.2, 8.1, and 10.9 μM, respectively. While, the IC_{50}(light) values of **MB** and **HMME** are either comparable with their MICs or even much lower, so they have no such a merit (Figure S8). Therefore, **P3** is more competitive to be an effective aPDT agent to selectively inactivate bacterial cells under conditions in which host tissues can be spared.

Conclusions

Three new cationic benzylidene cyclopentanone derivatives, **P1**, **P2**, and **P3**, were synthesized to study the selective photodynamic inactivation of bacteria over mammalian cells. The structure-antimicrobial property relationships of these PSs were discussed based on the influences of the modified charge numbers and positions of pyridyl cationic groups. It was found that **P1**-**P3** all presented much better aPDT effects compared to **MB** (cationic PS used in clinical practice) towards three strains and **HMME** (a second-generation porphyrin derivative used in clinic) towards *E. coli* (CA-31). Furthermore, compound **P3**, modified by two pyridyl groups unilaterally, was found perform best to inactivate not only standard strains but also the antibiotic-resistant *E. coli* (CA-31) with the MIC as low as 2.0 μM, at which about 94% mammalian cells were still viable, indicating its potential as aPDT agent to be used in clinic.

Acknowledgements

This work was supported by the National Natural Science Foundation of China (Grant No. 60978057). The authors are grateful to Dr. Meiling Zheng for her expertise assistance with the confocal fluorescence microscopy.

Notes and references

‡ Electronic Supplementary Information (ESI) available: [Characterization methods, ^{1}H NMR spectra of PSs, HPLC analysis of PSs, the measurement of singlet oxygen quantum yield in PBS, results of inhibition zones tests, MIC tests, cytotoxicity of **MB** and **HMME**, and cytotoxicity of new synthesized PSs toward B16 cells]. See DOI: 10.1039/x0xx00000x.

1. R. Ferraz, V. Teixeira, D. Rodrigues, R. Fernandes, C. Prudencio, J. P. Noronha, Z. Petrovski and L. C. Branco, *RSC Adv.*, 2014, **4**, 4301-4307.
2. V. Biju, *Chem. Soc. Rev.*, 2014, **43**, 744-764.
3. M. Ethirajan, Y. Chen, P. Joshi and R. K. Pandey, *Chem. Soc. Rev.*, 2011, **40**, 340-362.
4. G. Jori, C. Fabris, M. Soncin, S. Ferro, O. Coppellotti, D. Dei, L. Fantetti, G. Chiti and G. Roncucci, *Lasers Surg. Med.*, 2006, **38**, 468-481.
5. M. Yin, Z. Li, E. Ju, Z. Wang, K. Dong, J. Ren and X. Qu, *Chem. Commun.*, 2014, **50**, 10488-10490.
6. S. G. Awuah and Y. You, *RSC Adv.*, 2012, **2**, 11169-11183.
7. Q. Chen, J. Li, Y. Wu, F. Shen and M. Yao, *RSC Adv.*, 2013, **3**, 13835-13842.
8. A. Tavares, C. M. B. Carvalho, M. A. Faustino, M. G. P. M. S. Neves, J. P. C. Tomé, A. C. Tomé, J. A. S. Cavaleiro, Â. Cunha, N. C. M. Gomes, E. Alves and A. Almeida, *Mar. Drugs*, 2010, **8**, 91-105.
9. L. Costa, J. P. C. Tomé, M. G. P. M. S. Neves, A. C. Tomé, J. A. S. Cavaleiro, M. A. F. Faustino, Â. Cunha, N. C. M. Gomes and A. Almeida, *Antiviral Res.*, 2011, **91**, 278-282.
10. C. Bombelli, F. Bordi, S. Ferro, L. Giansanti, G. Jori, G. Mancini, C. Mazzuca, D. Monti, F. Ricchelli, S. Sennato and M. Venanzi, *Mol. Pharm.*, 2008, **5**, 672-679.
11. A. Frei, R. Rubbiani, S. Tubafard, O. Blacque, P. Anstaett, A. Felgenträger, T. Maisch, L. Spiccia and G. Gasser, *J. Med. Chem.*, 2014, **57**, 7280-7292.
12. P. A. C. Braga, A. Tata, V. Goncalves dos Santos, J. R. Barreiro, N. V. Schwab, M. Veiga dos Santos, M. N. Eberlin and C. R. Ferreira, *RSC Adv.*, 2013, **3**, 994-1008.
13. R. Bonnett, M. A. Krysteva, I. G. Lalov and S. V. Artarsky, *Water Res.*, 2006, **40**, 1269-1275.
14. M. A. Pereira, M. A. F. Faustino, J. P. C. Tome, M. G. P. M. S. Neves, A. C. Tome, J. A. S. Cavaleiro, A. Cunha and A. Almeida, *Photochem. Photobiol. Sci.*, 2014, **13**, 680-690.
15. J. Li, X. Liu, Y. Qiao, H. Zhu, J. Li, T. Cui and C. Ding, *RSC Adv.*, 2013, **3**, 11214-11225.
16. M. R. Hamblin and T. Hasan, *Photochem. Photobiol. Sci.*, 2004, **3**, 436-450.
17. H. Nikaido, *Science*, 1994, **264**, 382-388.
18. T. Maisch, R.-M. Szeimies, G. Jori and C. Abels, *Photochem. Photobiol. Sci.*, 2004, **3**, 907-917.

19. K. Li, W. Lei, G. Jiang, Y. Hou, B. Zhang, Q. Zhou and X. Wang, *Langmuir*, 2014, **30**, 14573-14580.
20. J. S. Friedberg, R. G. Tompkins, S. L. Rakestraw, S. W. Warren, A. J. Fischman and M. L. Yarmush, *Ann. N.Y. Acad. Sci.*, 1991, **618**, 383-393.
21. S. Gross, A. Brandis, L. Chen, V. Rosenbach-Belkin, S. Roehrs, A. Scherz and Y. Salomon, *Photochem. Photobiol.*, 1997, **66**, 872-878.
22. C. L. Zhu, Q. O. Yang, L. B. Liu, F. T. Lv, S. Y. Li, G. Q. Yang and S. Wang, *Adv. Mater.*, 2011, **23**, 4805-+.
23. Y. Zhao, W. Wang, F. Wu, Y. Zhou, N. Huang, Y. Gu, Q. Zou and W. Yang, *Org. Biomol. Chem.*, 2011, **9**, 4168-4175.
24. W. Yang, Q. L. Zou, Y. Zhou, Y. X. Zhao, N. Y. Huang, Y. Gu and F. P. Wu, *J. Photochem. Photobiol. a-Chem.,* 2011, **222**, 228-235.
25. S. Noimark, M. Bovis, A. J. MacRobert, A. Correia, E. Allan, M. Wilson and I. P. Parkin, *RSC Adv.*, 2013, **3**, 18383-18394.
26. J. P. Tardivo, A. Del Giglio, C. S. de Oliveira, D. S. Gabrielli, H. C. Junqueira, D. B. Tada, D. Severino, R. D. F. Turchiello and M. S. Baptista, *Photodiagnosis Photodyn. Ther.*, 2005, **2**, 175-191.
27. J. Sadaksharam, K. P. T. Nayaki and N. P. Selvam, *Photodermatol. Photoimmunol. Photomed.*, 2012, **28**, 97-101.
28. M. Wainwright, D. A. Phoenix, M. Gaskell and B. Marshall, *J. Antimicrob. Chemother.*, 1999, **44**, 823-825.
29. K.-H. Yuan, Q. Li, W.-L. Yu, D. Zeng, C. Zhang and Z. Huang, *Photodiagnosis Photodyn. Ther.*, 2008, **5**, 50-57.
30. Y. Gu, N. Y. Huang, J. Liang, Y. M. Pan and F. G. Liu, *Ann. Dermatol. Venereol.*, 2007, **134**, 241-244.
31. Y. Wang, Y. Wang, S. Wu and Y. Gu, *Optics in Health Care and Biomedical Optics Vi*, 2014, **9268**.
32. J. N. Demasa and G. A. Crosby, *J. Phys. Chem.,* 1971, **75**, 991-1024.
33. X.-L. Wang, Y. Zeng, Y.-Z. Zheng, J.-F. Chen, X. Tao, L.-X. Wang and Y. Teng, *Chem-a Eur. J.*, 2011, **17**, 11223-11229.
34. R. I. Lehrer, M. Rosenman, S. Harwig, R. Jackson and P. Eisenhauer, *J. Immunol. Methods*, 1991, **137**, 167-173.
35. T. Elavarasan, S. K. Chhina, M. Parameswaran Ash and K. Sankaran, *Sensor. Actuat. B-Chem.*, 2013, **176**, 174-180.
36. Q. Zou, Y. Fang, Y. Zhao, H. Zhao, Y. Wang, Y. Gu and F. Wu, *J. Med. Chem.,* 2013, **56**, 5288-5294.
37. J. Massin, W. Dayoub, J.-C. Mulatier, C. Aronica, Y. Bretonnière and C. Andraud, *Chem. Mater.*, 2010, **23**, 862-873.
38. X. Bai, L. Li, H. Liu, L. Tan, T. Liu and X. Meng, *ACS Appl. Mater. Interfaces,* 2015, **7**, 1308-1317.
39. V. Yarlagadda, P. Akkapeddi, G. B. Manjunath and J. Haldar, *J. Med. Chem.,* 2014, **57**, 4558-4568.
40. S. F. Nielsen, M. Larsen, T. Boesen, K. Schønning and H. Kromann, *J. Med. Chem.*, 2005, **48**, 2667-2677.
41. R. W. Redmond and J. N. Gamlin, *Photochem. Photobiol.*, 1999, **70**, 391-475.
42. S. J. Wagner, A. Skripchenko, D. Robinette, J. W. Foley and L. Cincotta, *Photochem. Photobiol.*, 1998, **67**, 343-349.
43. H. Lin, Y. Shen, D. Chen, L. Lin, B. C. Wilson, B. Li and S. Xie, *JFlu*, 2013, **23**, 41-47.
44. L. Shi, W. Zhang, K. Yang, H. Shi, D. Li, J. Liu, J. Ji and P. K. Chu, *J. Mater. Chem. B*, 2015, **3**, 733-737.
45. Thomas J. Dougherty, Charles J. Gomer, Barbara W. Henderson, Giulio Jori, David Kessel, Mladen Korbelik, Johan Moan and Q. Peng, *J. Natl. Cancer Inst.*, 1998, **90**, 889-905.

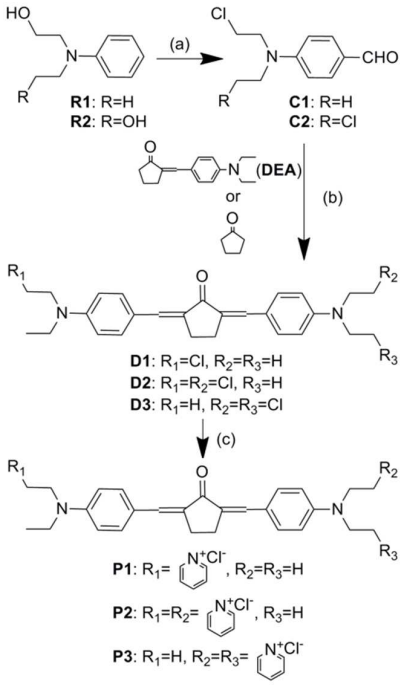

Scheme 1. Synthetic Routes of PSs **P1 – P3**. Conditions: (a) PCl_5, DMF, 45°C, 12 h; (b) MeOH, $LiOH{\cdot}H_2O$, 35 °C, 18 h; (c) Pyridine, 100°C, 24 h.

Table 1. Solubility, octanol-water partition coefficient, photophysics, and singlet oxygen production of PSs[a]

PS	Solubility (mg mL^{-1})	log P	λ_{max}^{ab} (nm)	ε_{max} (10^4 M^{-1} cm^{-1})	λ_{max}^{fl} (nm)	Φ_f	Φ_Δ
P1	4.3	1.8	501	4.1	643	0.015	0.036
P2	>10	-1.0	489	5.9	623	0.024	0.007
P3	>10	-0.1	498	4.5	630	0.015	0.027

[a]The solvent was phosphate buffered saline (PBS) unless otherwise noted; Log P is the octanol-water partition coefficient. λ_{max}^{ab} is the absorption maximum. ε_{max} is the molar absorption coefficient at λ_{max}^{ab}. λ_{max}^{fl} is the fluorescence emission maximum. Φ_f is the fluorescence quantum yield. Φ_Δ is the singlet oxygen quantum yield measured by photochemical trap method in PBS, Rose Bengal (RB) is used as the reference (Φ_Δ = 0.75 in PBS).

Table 2. The results of minimum inhibitory concentration (MIC) test for aPDT and dark- and photo-cytotoxicity of PSs toward HepG2 cells

PS	MIC (μM)			IC_{50} (light)	IC_{50} (dark)
	S. aureus	*E. coli*	*E.coli* (CA-31)		
P1	2.0	4.0	8.0	4.4	33.5
P2	2.0	4.0	8.0	9.6	>40.0
P3	1.0	2.0	2.0	7.7	>40.0
MB	>32.0	>32.0	>32.0	7.8	40.0
HMME	1.0	2.0	>32.0	2.3	>40.0

IC_{50} is the concentration of the photosensitizer that is necessary to achieve 50% growth inhibition of HepG2 cells in the dark or after irradiation by 532 nm light.

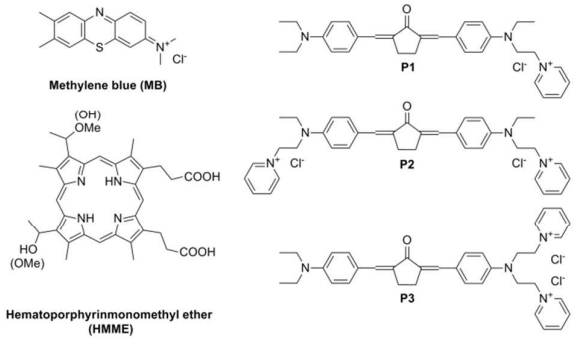

Figure 1. Chemical structures of **P1–P3**, **MB** and **HMME**.

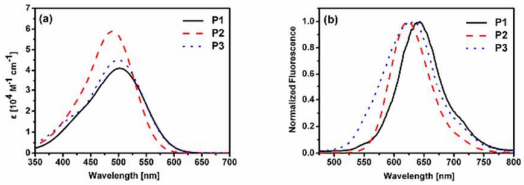

Figure 2. The UV-Vis absorption (a) and normalized fluorescence emission spectra (b) of **P1**-**P3** in PBS.

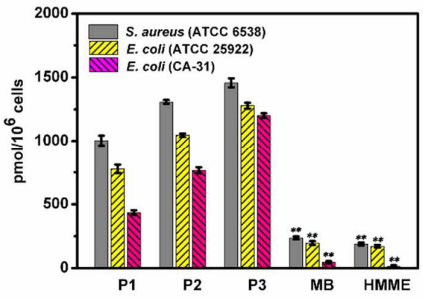

Figure 3. PS uptake by *S. aureus*, *E. coli*, and a drug resistant strain of *E. coli* (CA-31) after incubation with 10 μM PSs for 1h. (** $P < 0.05$ compared with the results of **P1**, **P2**, and **P3**).

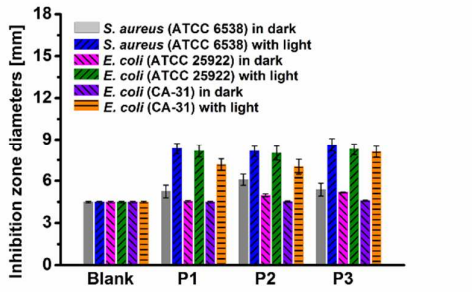

Figure 4. Diameters of the inhibition zone of PSs (4 μM) against *S. aureus*, *E. coli*, and *E. coli* (CA-31) after incubation for 24 h.

Journal Name

ARTICLE

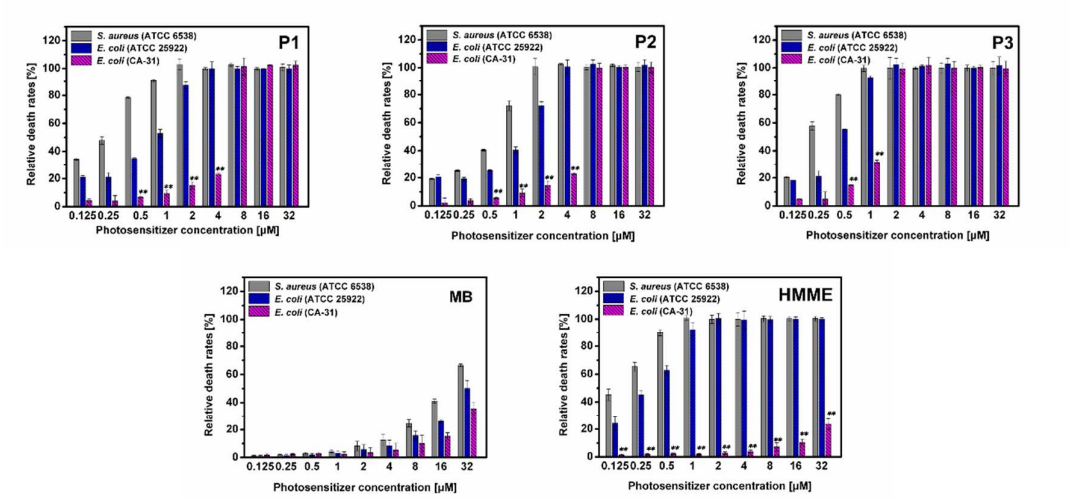

Figure 5. Relative death rate of three strains after being irradiated with laser (30 J cm^{-2}) for 10 min and incubated for another 24 h. (** $P < 0.05$ compared with the corresponding data of *S. aureus* and *E. coli*).

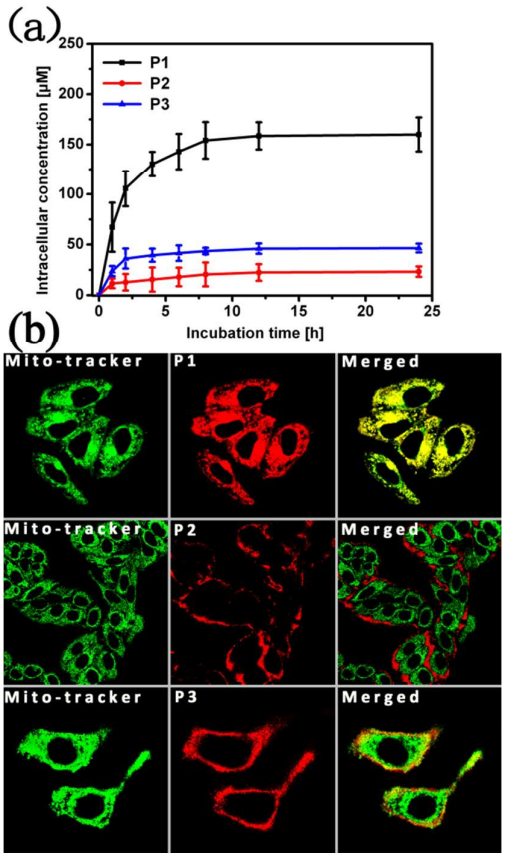

Figure 6. (a) PS uptake by HepG2 cells with 10 μM PSs for different times. The error bars denote the standard deviation of three replicates. (b) Confocal fluorescence images obtained by incubating HepG2 cells with 10 μM PSs for 8 h and 100 nM Mito-tracker green for 20 min.

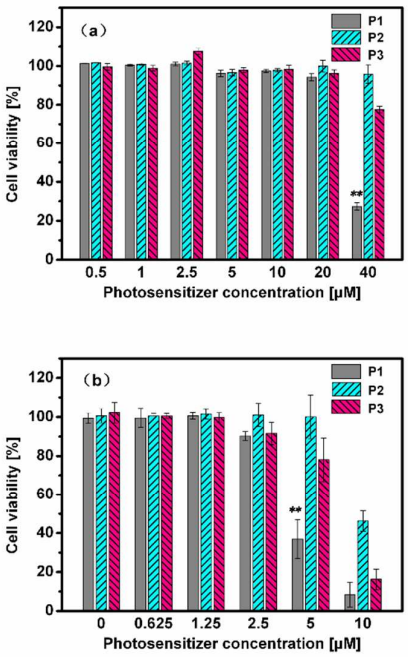

Figure 7. Viability of HepG2 cells incubated with different concentrations of PSs. (a) In dark. (b) Irradiated with a 532 nm laser (30 J cm^{-2}) for 10 min. (** $P < 0.05$ compared with the corresponding data of **P2** and **P3**).